Expression and Pharmacology of Endogenous Ca$_v$ Channels in SH-SY5Y Human Neuroblastoma Cells

Silmara R. Sousa, Irina Vetter, Lotten Ragnarsson, Richard J. Lewis*

Institute for Molecular Bioscience, The University of Queensland, St. Lucia, Australia

Abstract

SH-SY5Y human neuroblastoma cells provide a useful *in vitro* model to study the mechanisms underlying neurotransmission and nociception. These cells are derived from human sympathetic neuronal tissue and thus, express a number of the Ca$_v$ channel subtypes essential for regulation of important physiological functions, such as heart contraction and nociception, including the clinically validated pain target Ca$_v$2.2. We have detected mRNA transcripts for a range of endogenous expressed subtypes Ca$_v$1.3, Ca$_v$2.2 (including two Ca$_v$1.3, and three Ca$_v$2.2 splice variant isoforms) and Ca$_v$3.1 in SH-SY5Y cells; as well as Ca$_v$ auxiliary subunits $\alpha_2\delta_{1-3}$, β_1, β_3, β_4, γ_1, γ_{4-5}, and γ_7. Both high- and low-voltage activated Ca$_v$ channels generated calcium signals in SH-SY5Y cells. Pharmacological characterisation using ω-conotoxins CVID and MVIIA revealed significantly ($\sim$ 10-fold) higher affinity at human versus rat Ca$_v$2.2, while GVIA, which interacts with Ca$_v$2.2 through a distinct pharmacophore had similar affinity for both species. CVID, GVIA and MVIIA affinity was higher for SH-SY5Y membranes vs whole cells in the binding assays and functional assays, suggesting auxiliary subunits expressed endogenously in native systems can strongly influence Ca$_v$2.2 channels pharmacology. These results may have implications for strategies used to identify therapeutic leads at Ca$_v$2.2 channels.

Introduction

Voltage-gated Ca^{2+} channels (Ca$_v$) are membrane proteins essential for the control of calcium signaling events, such as muscle contraction, gene expression, and neurotransmitter and hormone release. Dysfunction of Ca$_v$ channels is related to a variety of heart, circulatory and neurological diseases; including arrhythmias, hypertension, some forms of epilepsy, migraine and other chronic diseases such as cancer, diabetes, ischemic brain injury and neuropathic pain [1,2]. The Ca$_v$ α subunit contains the voltage sensor and gating machinery and is the binding site for most inhibitors. This subunit comprises 4 domains each with six transmembrane segments. The pore is formed by the S5/S6 segments and the connecting pore loop, with channel opening gated by bending of the S6 segments at a hinge glycine or proline residue [3,4]. The voltage sensor domain consists of the S1–S4 segments, with positively charged residues in S4 serving as gating charges [5] (for review see: [3,6,7]).

Based on the distinct pharmacological and electrophysiological properties of Ca$_v$ channels, ten different gene subfamilies have been identified in vertebrates and classified as high voltage activated (HVA) Ca$_v$1.1–4 (L-type), Ca$_v$2.1 (P/Q-type), Ca$_v$2.2 (N-type), Ca$_v$2.3 (R-type); and low voltage activated (LVA) Ca$_v$3.1–3 (T-type). The α subunit includes channels containing α_{1S}, α_{1C}, α_{1D}, and α_{1F}, which mediate L-type Ca^{2+} currents. The Ca$_v$2 subfamily (Ca$_v$2.1 to Ca$_v$2.3) includes α subunits α_{1A}, α_{1B}, and α_{1E}, which mediate P/Q-type, N-type, and R-type Ca^{2+} currents, respectively. The Ca$_v$3 subfamily (Ca$_v$3.1 to Ca$_v$3.3) includes α subunits α_{1G}, α_{1H}, and α_{1L}, which mediate T-type Ca^{2+} currents

(**Table 1**) (for reviews see: [3,8,9]). Of these, Ca$_v$2.2 has been of particular interest as a therapeutic target given the central role it plays mediating neurotransmitter release in nociceptive pathways such as presynaptic nerve terminals and dendrites [10]. Ca$_v$ α subunits are co-expressed in native systems together with two or three auxiliary subunits (β, $\alpha_2\delta$ and γ), which undergo alternative splicing (for review see: [9]) and dramatically influence Ca$_v$ channel function, intracellular trafficking and posttranslational modifications [11]. Indeed, when expressed alone in recombinant system, the α_{1B} subunit, for example, encodes a voltage-dependent calcium channel with kinetic properties different from those of native Ca$_v$2.2 channels [9,12]. In contrast, when co-expressed with auxiliary β and $\alpha_2\delta$, increased current amplitudes are observed and the kinetics of activation and inactivation are closer to those of native channels [12].

Cell-based systems are desirable in the field of high-throughput screening assays due to their similarity to *in vivo* environment. SH-SY5Y human neuroblastoma cells are derived from human sympathetic neuronal tissue. This cell line maintains in culture many of the properties of nerve cells, providing a useful model for the characterisation of molecules affecting human neuronal function, including endogenously expressed Ca$_v$ channels [13–15]. In particular, SH-SY5Y cells have been an attractive model system for the study of Ca$_v$2.2 function [13]. Although heterologous expression models provide control of subunit expression, native systems provide potentially more complex models which, when characterized, can help to determine the pharmacology of drugs in a native context and the physiology and pathophysiology

Table 1. Primers used to identify Ca$_v$ channels α subunits in SH-SY5Y cells.

Subtype	Accession Number	Primer Forward/Reverse	Size (bp)	Annealing T (°C)
Ca$_v$1.1	NM_000069.2	CGCATCGTCAATGCCACCTGGTTTA/AGCACATTGTCGAAGTGGAAGTCGC	623	(?) ND
Ca$_v$1.2	[19]	CTGCAGGTGATGATGAGGTC/GCGGTGTTGTTGGCGTTGTT	502	58 [19]
Ca$_v$1.3	EU 363339.1	ACCCCCACCTGTAGGATCTCTCTCC/TCCTGACACTAGTCGAAGTGGTCGC	541	68
Ca$_v$1.3	NM_001128840.1	GCTGCTGTGGAAGTCTCTGTCAAGC/TCAGTGATTCCACCACACACCACGA	343	68
Ca$_v$1.4	NM_005183.2	AGGGACCCCTAAGCGAAGAAACCAG/ACCCCATGGCATCTTGCATCCAGTA	899	(?) ND
Ca$_v$2.1	FJ040507.1	AGGACGAGGACAGTGATGAA/GCAGAGGAAGATGAAGGA AA	365	(?) ND
Ca$_v$2.2	NM_000718.2	GGAACTGACTTCGACCTGCGAACAC/CCTCCTCTGCGTGGATCAGGTCATT	754	60
α$_{1B}$Δ$_1$	Bp 22+34	AGGAGATGGAAGAAGCAGCCAATCA/CCTTTCTGGTGTTTCATCTGGTGCA	900	58
α$_{1B}$Δ$_1$	Bp 23+33 [16]	CCAGAGGATGCAGACAATCAGCGGA/GCATCTTCTACCTGTCGAGGTACGC	900	60
α$_{1B}$Δ$_2$	Bp 21+31	CAGCCAATCAGAAGCTTGCTCTGCAAAAG/CTTTCGTTTGCGGTGGTCCCGCGGT	700	(65)
α$_{1B}$Δ$_2$	Bp 24+33 [16]	CAAGGATGAAGAGGAGATGGAAGAA/GCGTACCTCGACAGGTAGAAGATGC	1300	(?) ND
Ca$_v$3.1	BC110995.1	GCTGCTGGAGACACAGAGTACAGGT/CTCGTGGTATTCGATGCCCATGCTG	397	60
Ca$_v$3.2	NM_021098.2	CCTGATCCCTACGAGAGATCCCGC/CACGGCTGAAGTACTTGCTGTCCAC	433	60
Ca$_v$3.3	AF393329.1	AGATGCCCTTCATCTGCTCCCTGTC/AAGATCTCCTCGTAGCAGTCGCCAG	526	60

(?) ND: isoform not detected, unknown annealing temperature.
doi:10.1371/journal.pone.0059293.t001

of endogenously expressed receptors and channels. However, little is known about the Ca$_v$ subtypes and auxiliary subunits endogenously expressed in SH-SY5Y cells, limiting the interpretation of pharmacological data. Here we report a detailed characterisation of endogenously expressed Ca$_v$ channels expressed in SH-SY5Y cells using PCR and pharmacological approaches, with particular emphasis on the nociceptive target Ca$_v$2.2.

Results

SH-SY5Y Cells Endogenously Express Multiple Ca$_v$ Subtypes, Ca$_v$2.2 Isoforms and Auxiliary Subunits

We assessed expression of mRNA transcripts for Ca$_v$ subtypes and auxiliary α$_2$δ, β and γ subunits isoforms in SH-SY5Y cells by performing RT-PCR using specific primers (**Fig. 1A–D**). Bands with the predicted sizes were detected for Ca$_v$1.3, Ca$_v$2.2, and Ca$_v$3.1, while Ca$_v$1.1, 1.2, 1.4, 2.1, 2.3, 3.2 and 3.3 were not detected (**Fig. 1A**). In addition, bands of expected sizes for (**Table 2**) β$_1$, β$_3$, β$_4$, α$_2$δ$_{1-3}$, γ$_1$, γ$_4$, γ$_5$ and γ$_7$ auxiliary subunits (**Fig. 1C–D**) were also identified. Since splice variants can be generated by alternative RNA processing, which can influence function and pharmacology [16], we also investigated the expression of some human splice variants [16,17]. PCR bands with the predicted sizes for Ca$_v$1.3 isoforms 1 and 2; full length Ca$_v$2.2, α$_{1B1}$ (Gene bank accession number M94172.1), shorter α$_{1B}$ variant, α$_{1B2}$ (Gene bank accession number M94173.1) [17]; and Δ$_1$ (but not Δ$_2$) [16,18] were detected for the first time in the SH-SY5Y cells (**Fig. 1A, Table 1**).

The best annealing temperature for each gene analysed (see **Table 1–2**) was determined using a gradient PCR protocol in rounds of control experiments prior to testing each Ca$_v$ gene-specific primer. Target-specific primers for the housekeeping gene GAPDH were designed as previously described [19] and GAPDH was detected in all PCRs, indicating amplifications were cDNA specific. PCR master mix using random primers without cDNA was used as negative gDNA control in all PCRs. Specificity of primers was demonstrated in a range of control experiments (data not shown), including detection of Ca$_v$2.2 plasmid but not other

Ca$_v$ subtypes by Ca$_v$2.2 primers; and absence of Ca$_v$2.2 in HEK cells. β$_1$ and α$_2$δ$_1$ primers were positive for β$_1$ and α$_2$δ$_1$ plasmids, while the same primers were negative for β$_{2-4}$ and α$_2$δ$_{2-4}$ (data not shown), indicating primers were selective for β$_1$ and α$_2$δ$_1$ auxiliary subunits. The identity of each of these PCR products, including γ$_1$, γ$_4$, γ$_5$ and γ$_7$, was confirmed by sequencing analysis (data not shown).

Displacement of ^{125}I-GVIA Binding from SH-SY5Y Cell Membranes

GVIA is a highly selective Ca$_v$2.2 blocker [20] and ^{125}I-GVIA binding assays have been well established using rat brain membranes [21–23]. We performed binding assays and confirmed SH-SY5Y cells contain ^{125}I-GVIA binding sites which can be fully displaced by Ca$_v$2.2 selective inhibitors ω-conotoxins CVID, GVIA and MVIIA. Affinities of ω-conotoxins for human and rat Ca$_v$2.2 channels were next compared using these assays. CVID, GVIA and MVIIA each fully displaced ^{125}I-GVIA binding to crude rat brain membranes with similar affinities (pIC$_{50}$± SEM values; CVID 10.53±0.15, GVIA 10.43±0.16, and MVIIA 10.19±0.04) (**Fig. 2A, Table 3**), consistent with earlier studies [21]. Intriguingly, the affinity of GVIA (pIC$_{50}$ 10.55±0.15) to displace ^{125}I-GVIA binding to SH-SY5Y membranes was similar to that shown in rat brain, while both CVID and MVIIA had significant higher affinity for the human cell membranes (pIC$_{50}$s of 11.51±0.12 and 11.29±0.23, respectively) than for rat brain membranes (**Fig. 2A, B and D, Table 3**). In addition, the affinities of these ω-conotoxins dramatically decreased when determined on the intact SH-SY5Y cells instead of membranes, with GVIA affinity shifted ~10-fold, and CVID and MVIIA affinity shifted ~100-fold (see **Fig. 2C, Table 3**).

Pharmacology of the Endogenously Expressed Ca$_v$ Channels

To investigate if the Ca$_v$ channels endogenously expressed in SH-SY5Y cells were functional, and to further study the pharmacology of these channels, we assessed KCl-evoked Ca$_v$ responses using a fluorescent high-throughput Ca^{2+} imaging assay
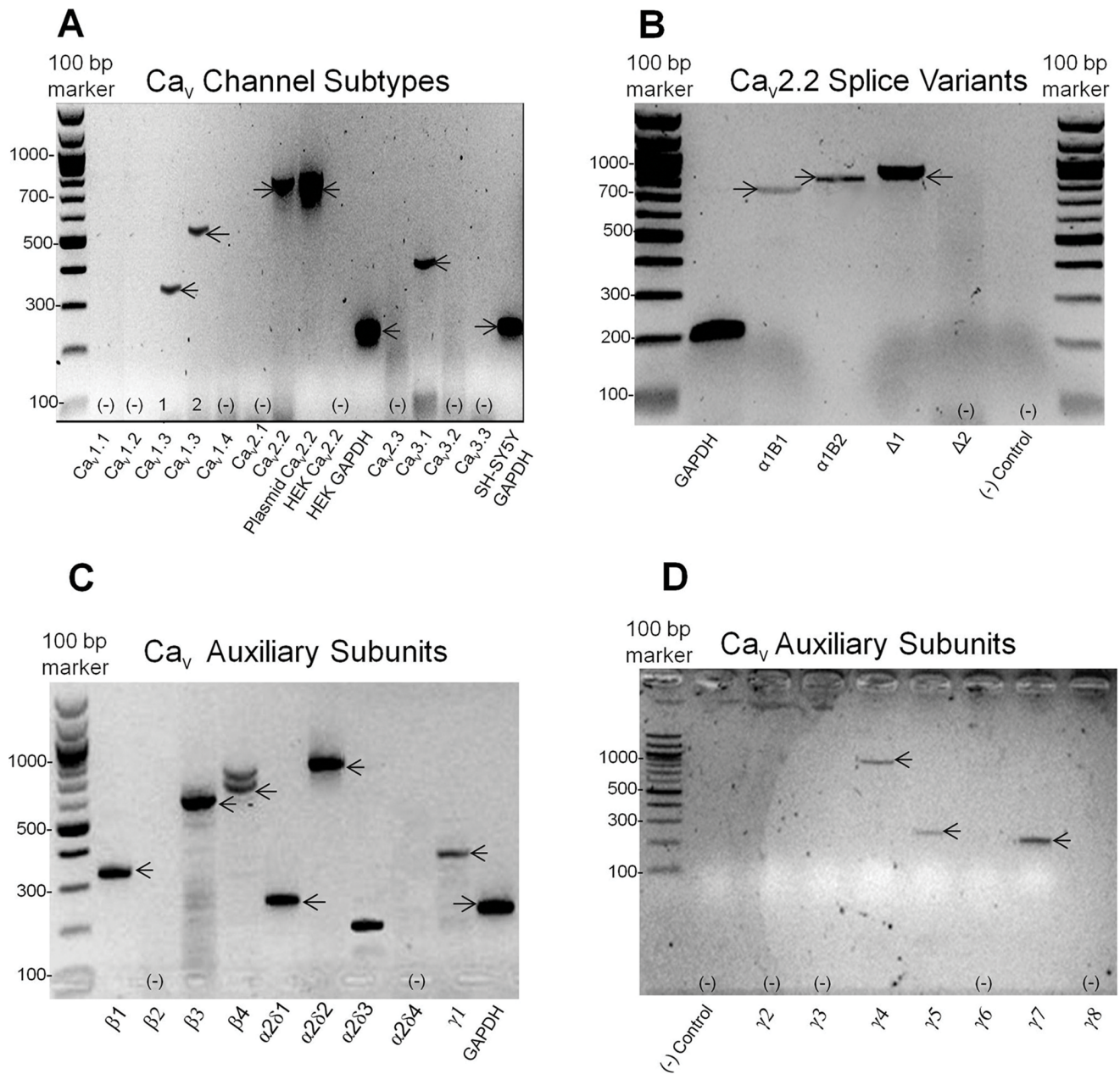
Figure 1. RT-PCR to identify the Ca$_v\alpha$ and auxiliary subunit isoforms expressed in SH-SY5Y cells. Expression of Ca$_v\alpha$ subtypes, auxiliary β, $\alpha_2\delta$ and γ subunits, as well as Ca$_v$2.2 splice variant isoforms were determined in SH-SY5Y cells using standard RT-PCR and specific primers for each isoform. (**A**) SH-SY5Y cells endogenously express Ca$_v$1.3 isoform 1, Ca$_v$1.3 isoform 2, Ca$_v$2.2 and Ca$_v$3.1, but not Ca$_v$1.1 and Ca$_v$1.2, Ca$_v$1.4, Ca$_v$2.3, Ca$_v$3.2 and Ca$_v$3.3. Expected band sizes were (bp): Ca$_v$1.3 isoform 1, 541; Ca$_v$1.3 isoform 2, 343; Ca$_v$2.2, 754; and Ca$_v$3.1, 397, as indicated with arrows (**B**) SH-SY5Y cells endogenously express different Ca$_v$2.2, α_{1B} splice variant isoforms. Bands with predicted sizes were (bp): α_{1B1}, 728; α_{1B2}, 854; Δ_1, 900 bp. No band was detected for splice Δ_2. (**C–D**) SH-SY5Y cells express the auxiliary β_1, β_3, and β_4 but not β_2; in addition to $\alpha_2\delta_{1–3}$, but not $\alpha_2\delta_4$; and γ_1, $\gamma_{4–5}$ and γ_7 but not $\gamma_{2–3}$ and γ_8 subunits. Expected band sizes were (bp, base pairs): β_1, 331; β_3, 594; β_4, 731; $\alpha_2\delta_1$, 252; $\alpha_2\delta_2$, 878; $\alpha_2\delta_3$, 132 and γ_1, 367; γ_4, 909; γ_5, 257; and γ_7, 910.
doi:10.1371/journal.pone.0059293.g001

on the FLIPR$^{\text{Tetra}}$ (Fluorescent plate image reader, Molecular Devices, Sunnyvale, CA) (**Fig. 3A–D**). CaCl$_2$ (5 mM) was added to the KCl stimulation solution in all experiments to maximize the Ca^{2+} influx signal. Co-addition of 90 mM KCl and 5 mM CaCl$_2$ evoked a large transient response indicating increase in intracellular Ca^{2+} (**Fig. 3A–B**). Concentration-response curves for KCl-mediated stimulation showed activation of Ca$_v$ responses with an EC$_{50}$ of 17.3 mM (pEC$_{50}$ 1.88±0.06, Hill slope of 2.5) (**Fig. 3A,**

Table 4), similar to previously described values [24–26]. To assess the contribution of each Ca$_v$ channel expressed in SH-SY5Y cells to the KCl-evoked Ca^{2+} responses, we determined concentration-response curves for KCl/Ca^{2+} stimulation in the presence of subtype-specific inhibitors. The Ca$_v$1 (L-type) inhibitor nifedipine was used at a concentration (10 μM) that does not affect responses of other Ca$_v$ subtypes (N, R, P/Q or T-type) [27], to isolate non-L-type responses. The KCl concentration-response curve was shifted

Table 2. Primers used to identify Ca$_v$ channel auxiliary subunits in SH-SY5Y cells.

Subunit	Accession Number	Primer Forward/Reverse	Size (bp)	Annealing T (°C)
β_1	NM_000723.3	ATGCACGAGTACCCAGGGGAG/CAGCGCAGTAGCGGGCCTTATT	331	60
β_2	NM_000724.3	TCGCTTGCCAAACGCTCGGT/ATGACGGCTGCGCTGCTTGT	909	(?) ND
β_3	NM_000725.2	GCAGCAGCTCGAAAGGGCCA/ATGCTGGAGCGGGCAGAGGA	594	65
β_4	NM_001005747.2	TGAAGACTCGGAGGCTGGTTCAGC/TGGACCGGGTGTTCGAACGT	731	(?) ND
$\alpha_2\delta_1$	NM_000722.2	TGCTCATCGGCCCCTCGTCG/CCAGGCGCACCAGGGCTTTAG	252	60
$\alpha_2\delta_2$	NM_001174051.1	AGCCTAGGCAGGCGCACACT/TCTGCACTAGCTCACACTGCTCCGG	878	60
$\alpha_2\delta_3$	NM_018398.2	GGACGAGAGGCTGCGTTTGCA/GGGCCGGCTAAGCACGTGAA	132	65
$\alpha_2\delta_4$	NM_172364.4	TGGCCTGGGCCTTTGTGCAG/GCCTCCTCGGCAGCTTCCAC	328	(?) ND
γ_1	NM_000727.3	TGCTGGCCATGACAGCCGTG/AACATGGACGCGGGTCGCAG	367	60
γ_2	NM_006078.3	TCTCTGGGCCTTAATTTTCCCC/TTTTCACAGACCCCCAAAGACA	439	(?) ND
γ_3	NM_006539.3	CTCCCCTTCCCCTTTCCTTAAC/AGCTGGGATTTCCTTTCTGGAG	840	(?) ND
γ_4	NM_014405.3	TTTGCACGAAGGTTGTGCTG/TTGCTCTCCTGGCGTTGATT	909	62–64
γ_5	NM_145811.2	GATCAAGATGTCCCTGCACTCA/CAGAGACAAAGGCCAGTATCGT	257	64
γ_6	NM_145814.1	TGCTCAGTAAAGGTGCAGAGTT/CTCGGTGGTTGCTTAGAGAAGT	334	(?) ND
γ_7	NM_031896.4	ACTGGCTGTACATGGAAGAAGG/TGAAATAAGGGAGTCTGTGGGC	910	65
γ_8	NM_031895.5	TGCTGAAGCATAGTCATGGTGT/CCTCTGCCTTCTCAGTGAACTT	987	(?) ND

(?) ND: isoform not detected, unknown annealing temperature.

to the right in the presence of nifedipine (EC$_{50}$ of 20.4 mM, pEC$_{50}$ 1.69±0.12, Hill slope of 2.9) (**Fig. 3A Table 4**). Conversely, the Ca$_v$2.2 (N-Type) inhibitor ω-conotoxin CVID was used at a concentration that does not affect responses of other Ca$_v$s (up to 3 µM) [21,28], to isolate non-N-type responses. Compared to responses in the presence of nifedipine, the KCl concentration-response curve was shifted to the left in the presence of CVID (EC$_{50}$ of 18.6 mM, pEC$_{50}$ 1.86±0.10, Hill slope of 3.5) (**Fig. 3A, Table 4**). These differences can be accounted for by the electrophysiological properties of each Ca$_v$ channel subtype identified, since L-type requires a larger depolarization than N-type to be activated [28], and the control KCl responses is a result of activation of both channel types. These results confirm that SH-SY5Y cells express functional Ca$_v$ subtypes, including Ca$_v$1 and Ca$_v$2.2, which can be pharmacologically isolated using selective inhibitors. The observed pharmacology is consistent with the subtypes identified in our PCR experiments and with previous reported electrophysiological data [14,15].

Since 90 mM KCl/5 mM CaCl$_2$ elicits maximal Ca$_v$1 and Ca$_v$2.2 responses (**Fig. 3A**), we used this combination to further characterize the Ca$_v$ channel subtypes expressed in SH-SY5Y cells. Concentration-response curves for nifedipine at Ca$_v$1 channels were generated in the presence of saturating concentration of CVID (3 µM). Under these conditions, nifedipine inhibited KCl evoked Ca^{2+} responses with an IC$_{50}$ of 0.28 µM (pIC$_{50}$ 6.5±0.052) (**Fig. 3C, Table 4**), consistent with reports for nifedipine block of L-type responses in neuronal cells [29]. To characterize Ca$_v$2.2 pharmacology, inhibition by ω-conotoxins was determined in the presence of a near saturating concentration of nifedipine (10 µM). Under these conditions, the potency of CVID was IC$_{50}$ 0.16 µM (pIC$_{50}$ 6.87±0.078), GVIA 0.15 µM (pIC$_{50}$ 6.84±0.06) and MVIIA 0.024 µM (pIC$_{50}$ 7.7±0.13) (**Fig. 3D, Table 4**). These results are consistent with previous studies on MVIIA [22–24,26] and CVID [22–24] inhibition of N-type responses in native and recombinant systems, when Ca$_v$2.2 was co-expressed with β and α$_2$δ subunits [22–24]. In contrast, GVIA potency at Ca$_v$2.2 expressed in SH-SY5Y cells (IC$_{50}$ of

0.15 µM; pIC$_{50}$ 6.8±0.072) was consistently lower than previously described for heterologous expressed rat [24,26] and human [25] α$_{1B}$ co-expressed with α$_2$δ$_1$ and β$_3$, but similar to data obtained using native expression systems such as dissociated rat DRG cells [30] and chicken synaptosomes [31].

A small portion (5–15%) of the KCl-evoked responses was insensitive to block by co-application of 10 µM nifedipine and 3 µM CVID (**Fig.3C–D**). To pharmacologically characterize these remaining responses, we assessed the effects of Ca$_v$2.1 and Ca$_v$2.3 subtype-specific inhibitors, as well as of compounds with activity at Ca$_v$3, on the Ca^{2+} responses evoked by 90 mM KCl/5 mM CaCl$_2$, in the presence of both CVID and nifedipine. The Ca$_v$2.1 blockers ω-agatoxin IVA (data not shown) and ω-agatoxin TK did not significantly affect KCl-evoked Ca^{2+} responses at concentrations up to 10 µM (**Fig. 4A–B, Table 4**). The Ca$_v$2.3 antagonist SNX 482 also had no significant inhibitory effect at concentrations up to 10 µM (**Fig. 4A and C, Table 4**). On the other hand, mibefradil (30 µM), a benzimidazolyl-substituted tetraline reported to inhibit Ca$_v$3 responses in different systems with weak affinity [32,33] fully inhibited these remaining responses with an IC$_{50}$ of 3 µM (pIC$_{50}$ 5.3±0.035) (**Fig. 4A and D, Table 4**). Similar IC$_{50}$ values for mibefradil block of T-type responses in native systems have been previously reported (see [32–35]). In addition, another Ca$_v$3 inhibitor, the antipsychotic pimozide, also fully inhibited the remaining responses with an IC$_{50}$ of 1.3 µM (pIC$_{50}$ 5.2±0.097) (**Fig. 4A, Table 4**), similar to previously reported literature values [34]. These findings are in agreement with our PCR (**Fig. 1A–B**) which detected mRNA transcripts for Ca$_v$3.1, but neither Ca$_v$2.1 nor Ca$_v$2.3 was identified.

Discussion

Ca$_v$2.2 channels play a key role in regulating nociception. Inhibition of Ca$_v$2.2 at the spinal cord produces analgesia in animal models of pain [23,36] and in humans [37], with direct (eg. Prialt) and indirect (eg. gabapentin) inhibitors among some of the
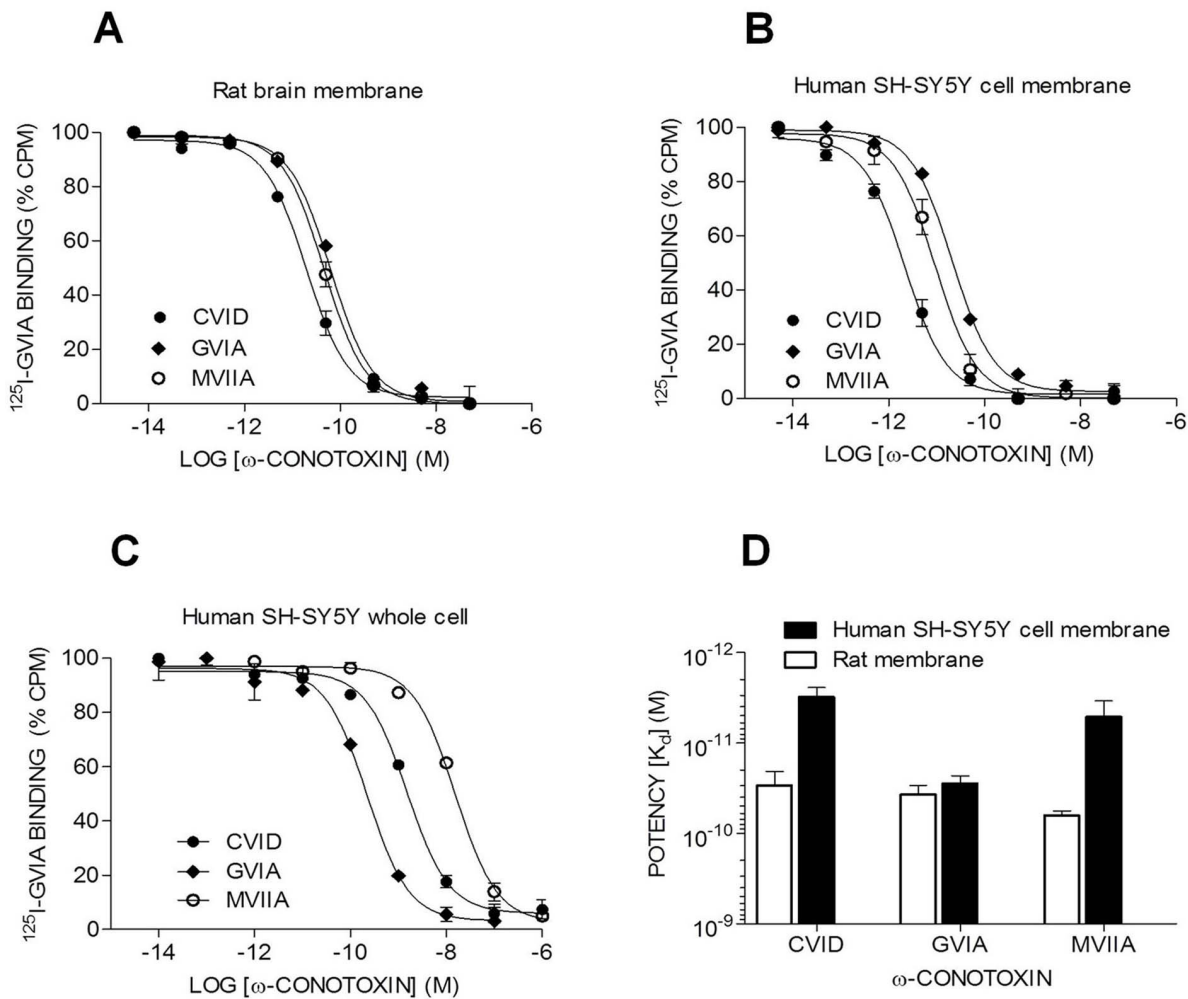
Figure 2. Displacement of ^{125}I-GVIA from SH-SY5Y whole cell and membranes by ω-conotoxins. Displacement of ^{125}I-GVIA binding to Ca$_v$2.2 expressed in rat brain and SH-SY5Y intact/whole cell and membranes. (**A**) Displacement of ^{125}I-GVIA from rat brain membranes. (**B**) Displacement of ^{125}I-GVIA from human SH-SY5Y cell membranes. (**C**) Displacement of ^{125}I-GVIA from human SH-SY5Y whole cell. (**D**) ω-Conotoxins affinity (K$_d$ ± SEM) to displace ^{125}I-GVIA from rat brain membranes and human SH-SY5Y cell membranes. Data are mean ± SEM of triplicate data from a representative experiment best fitted to a single-site competition model using GraphPad Prism.
doi:10.1371/journal.pone.0059293.g002

most recently developed analgesics [18]. Neuroblastoma cells, including the sympathetically derived human neuroblastoma cell line SH-SY5Y, provide excellent model systems to study Ca$_v$2.2 channels in a native context [14,15]. However little is known about the Ca$_v$α and auxiliary subunits expressed, limiting interpretation of pharmacological data from these cells. To address this limitation, we have characterized the expression and pharmacology of Ca$_v$ channels in SH-SY5Y cells and investigated mechanisms likely to influence the pharmacology of ω-conotoxins at Ca$_v$2.2 channels.

Previous electrophysiological studies have identified L- and N-currents from high voltage activated channels Ca$_v$1 and Ca$_v$2.2 in SH-SY5Y cells, but not low voltage activated T- type currents from Ca$_v$3 channels [13–15,38]. In contrast, we detected mRNA transcripts for the N-type (Ca$_v$2.2), two L-type (Ca$_v$1.3 isoform 1 and 2) and one T-type isoform (Ca$_v$3.1). In addition, we also detected mRNA transcripts for Ca$_v$2.2 splice variants, including α$_{1B2}$ (74 amino acid shorter) [16,17,39] and the splice α$_{1B}$Δ$_1$ (382 amino acid shorter) [16].

Functional Ca$_v$ responses elicited by addition of KCl/CaCl$_2$ were assessed using a fluorescent high-throughput Ca^{2+} imaging assay on the FLIPR^{Tetra}. KCl has been used extensively to activate Ca$_v$ responses in a diversity of functional assays ([24,26,40]). Addition of high concentrations of KCl causes a change in membrane potential, which in turn leads to opening of Ca$_v$ channels, influx of Ca^{2+} and a resultant increase in intracellular fluorescence. While the change in membrane potential elicited by addition of KCl at the concentrations used here is approximately linear, accumulation of intracellular Ca^{2+} is saturable and fits a sigmoidal concentration-response curve because a change in membrane potential leads to a finite change in channel open probability and thus Ca^{2+} influx.

Ca$_v$2.2 channels expressed in SH-SY5Y cells were functional and generated KCl activated responses that were inhibited by ω-conotoxins CVID, GVIA and MVIIA in the presence of saturating concentrations of nifedipine. As expected, when L-type responses were isolated by addition of saturating concentrations of CVID, nifedipine concentration-dependently blocked KCl responses. However, a small response remained (5–15%) in the presence of
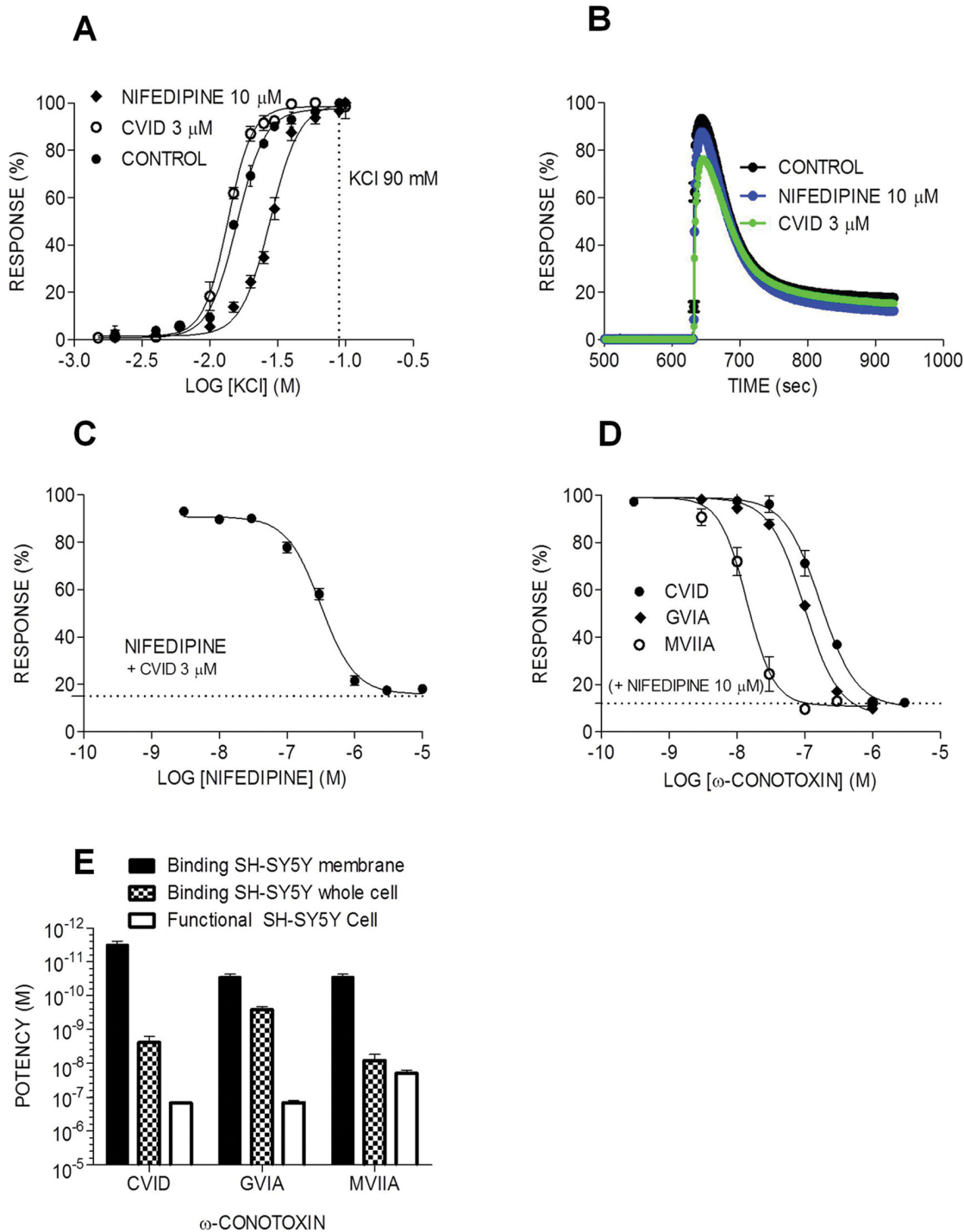
Figure 3. Ca$_v$2.2 and Ca$_v$1 channels endogenously expressed in SH-SY5Y cells are functional. Data obtained from fluorescent Ca^{2+} imaging assays of KCl-evoked Ca^{2+} responses in SH-SY5Y cells. **(A)** Ca$_v$1 and Ca$_v$2.2 activation in the presence of CVID (open ball) and nifedipine (filled ball), respectively, shifted control KCl-evoked Ca^{2+} responses (quadrilateral) significantly in SH-SY5Y cells ($p > 0.05$). **(B)** Time course of Ca^{2+} responses is shown for control KCl 90 mM (black), KCl in the presence of nifedipine (blue) and KCl in the presence of CVID (green). **(C)** Concentration-response curve for nifedipine inhibition of Ca$_v$1 responses **(D)** Concentration-response curves for CVID, GVIA and MVIIA inhibition of Ca$_v$2.2 responses. The responses were normalized using controls: positive KCl and negative PSS buffer; and plotted across increasing concentrations of antagonists **(E)** Comparison of ω-conotoxins CVID, GVIA and MVIIA potencies (IC$_{50}$/K$_d$ ± SEM of n = 3–4 replicates for each experiment, n = 3 experiments) in displacing ^{125}I-GVIA from SH-SY5Y whole cell and SH-SY5Y cell membranes with the functional assays data.
doi:10.1371/journal.pone.0059293.g003

a combination of Ca$_v$2.2 and Ca$_v$1 inhibitors. This resistant response was completely abolished by the Ca$_v$3 inhibitors mibefradil and pimozide. While mibefradil and pimozide are not specific inhibitors of T-type currents and also inhibit L-type channels [32,41], inhibition of the residual Ca^{2+} response was also observed in the presence of saturating concentrations of nifedipine,

Table 3. ω-Conotoxin affinities (IC$_{50}$± SEM) to displace ^{125}I-GVIA binding.

ω-Conotoxin	Rat membrane K$_d$ (nM)	SH-SY5Y membrane K$_d$ (nM)	Whole SH-SY5Y K$_d$ (nM)
CVID	0.034±0.013	0.0034±0.009	3.2±0.2
GVIA	0.043±0.013	0.033±0.012	0.27±0.084
MVIIA	0.064±0.007	0.0065±0.0019	10±0.085

doi:10.1371/journal.pone.0059293.t003

suggesting that activity of these compounds at L-type channels did not contribute to inhibition of residual response. Based on our observations that this resistant response was not blocked by inhibitors of L-type (nifedipine), N-type (CVID), R-type (SNX 482) or P/Q-type channels (ω-agatoxin), but was completely abolished by compounds with known activity at T-type channels, it seems plausible that this response may be mediated by Ca$_v$3.1, which mRNA expression was detected in SH-SY5Y. Alternatively, it is known that the Δ_1 splice variant, which mRNA expression was detected in SH-SY5Y cells, is significantly more resistant to the blockade by MVIIA and GVIA [42]. While inhibition by CVID of the Ca$_v$2.2 splice variants detected in SH-SY5Y cells has not been characterised, it is possible that, akin to inhibition of Na$_v$ channels by the μ-conotoxin GIIIA, complete current inhibition by CVID cannot be achieved for these splice variants. Alternatively, the response remaining in the presence of nifedipine and CVID could represent another undefined resistant current, or an artifact of the KCl/Ca^{2+} activation buffer used in this study.

Development of non-electrophysiological HTS Ca$_v$3 channel assays has been hampered by some of the properties of this channel, including their low voltage threshold for activation and inactivation and rapid inactivation kinetics. However, although T-type currents inactive rapidly, fluorescence Ca^{2+} assays detect accumulation of intracellular Ca^{2+} rather than currents, and are thus not subject to the same temporal resolution constraints. In addition, compared to heterologous systems, SH-SY5Y cells have a relatively hyperpolarised resting membrane potential [43], which would be conducive to channels being present in the resting state. Accordingly, Ca^{2+} assays at Ca$_v$3 channels using the FLIPR have been successfully developed [40] and it is clearly conceivable that functional responses of Ca$_v$3.1 expressed in SH-SY5Y cells could be elicited using KCl/Ca^{2+} stimulation.

In addition to functional characterization, we also confirmed Ca$_v$2.2 expression at the protein level using ^{125}I-GVIA binding assays. The ω-conotoxins CVID, GVIA and MVIIA each fully displaced ^{125}I-GVIA binding to SH-SY5Y cell membranes with high affinity. Interestingly, while the affinity of GVIA was not significantly different between species, CVID and MVIIA affinities were ~10-fold higher in human SH-SY5Y membranes compared to rat brain membranes. These results support the findings that MVIIA and CVID interacts with Ca$_v$2.2 human channels through a different pharmacophore, as compared with GVIA [44].

Variation in the affinity of ω-conotoxins between species is likely influenced by Ca$_v$α splice variants, with differences in toxin sensitivity, time course and voltage-dependence of inactivation, single channels conductance, gating behavior and sensitivity to G-protein-mediated modulation reported for splice isoforms endogenously expressed in neuronal cells of rat, mouse, rabbit and humans [16,17,39,42,45–48] (for review see: [46]). In pain, the Ca$_v$2.2 splice variant 37a replaces the usual variant 37b in a specific subset of nociceptive neurons, and thus may represent a potential therapeutic target [42,46,49]. However, this variant has to date only been described in rat dorsal root ganglion neurons, and is not known to be present in human tissue.

Additional human splice variants include two α$_{1B}$ isoforms that have long or short C-termini [17], and two human forms that lack large parts of the domain II-III linker region, including the synaptic protein interaction site. These splice variants, termed Δ_1 and Δ_2, have been previously isolated from IMR32 human neuroblastoma cell line and human brain cDNA libraries [16]. We have identified mRNA transcripts for the full length α$_{1B1}$, α$_{1B2}$ (74 amino acid shorter) [16,17,39] and the splice variant Δ_1 (382 amino acid shorter) [16] in SH-SY5Y cells. The α$_{1B1}$ is an axonal/synaptic isoform, while α$_{1B2}$ is restricted to neuronal soma and

Table 4. Potency (IC$_{50}$± SEM) of Ca$_v$ channel modulators on functional assays.

Ca$_v$ Activator/Inhibitor	Ca^{2+} Stimulation EC$_{50}$ (mM)	Ca^{2+} Inhibition IC$_{50}$ (μM)
KCl	17.28±3.41	–
KCl+CVID	18.61±3.22	–
KCl+NIFEDIPINE	20.35±3.17	–
CVID	–	0.16±0.025
GVIA	–	0.15±0.09
MVIIA	–	0.024±0.005
NIFEDIPINE	–	0.23±0.046
MIBEFRADIL	–	3.0±0.031
PIMOZIDE	–	1.3±0.097
ω-AGATOXIN TK	–	NDR
SNX 482	–	NDR

NDR: Non-detectable response.
doi:10.1371/journal.pone.0059293.t004
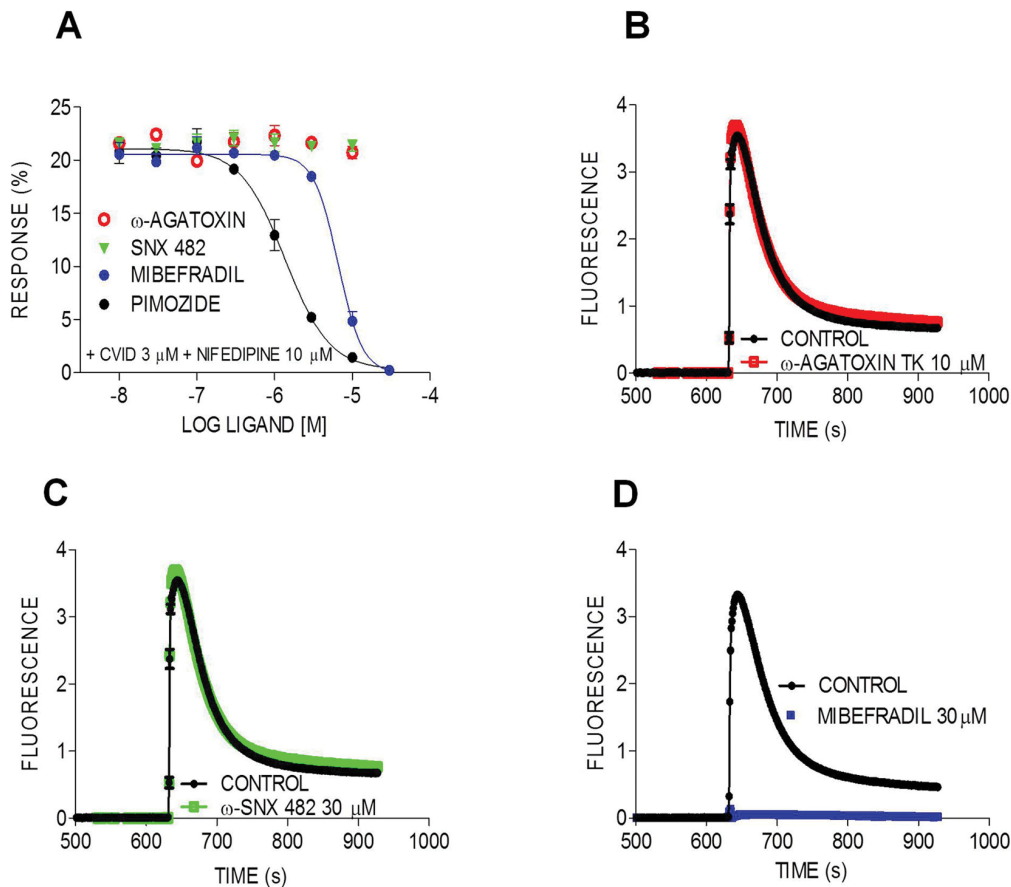
Figure 4. Characterization of resistant Ca^{2+} responses in SH-SY5Y cells. Data obtained from fluorescent Ca^{2+} imaging of KCl-evoked Ca^{2+} responses in SH-SY5Y cells. (**A**) Concentration-response curves for mibefradil, pimozide, ω-agatoxin TK and SNX 482 in inhibiting resistant KCl-evoked Ca^{2+} responses in SH-SY5Y cells, pretreated with CVID (3 μM) plus nifedipine (10 μM) (**B–D**) Time course of transient Ca^{2+} responses activated by 90 mM KCl/5 mM CaCl$_2$, in the presence of CVID (3 μM) and nifedipine (10 μM) and following the addition of agatoxin TK, SNX-482 and mibefradil.
doi:10.1371/journal.pone.0059293.g004

dendrites [39,50], however, apart from differential susceptibility to Gαi/Gαo-versus Gαq-mediated inhibition, little is known regarding its biophysical and pharmacological properties. On the other hand, the Δ$_1$ splice variant has lost part of the synaptic protein interaction (synprint) site and is thus unlikely to play a role in fast synaptic transmission, with shifts in the voltage dependence of steady-state inactivation and a more rapid recovery from inactivation compared to full length α$_{1B1}$ [16]. Importantly and clinically relevant, Δ$_1$ variant was significantly more resistant to the blockade by MVIIA and GVIA; however the degree of effect varied for each toxin [16]. Thus, expression of the Δ$_1$ variant in SH-SY5Y cells may contribute to the reduced ω-conotoxin affinity observed. While expression of these splice variants in SH-SY5Y cells was detected using gene specific primers, which have been extensively validated in the literature [17], further confirmation of expression at the protein level is warranted.

Ca$_v$ channel auxiliary subunits can also influence the pharmacology of Ca$_v$ inhibitors, with ω-conotoxins displaying reduced affinity in the presence of the α$_2$δ subunit [11,22–24,27,51]. Specifically ω-conotoxins GVIA, MVIIA and CVID had reduced affinity when α$_2$δ$_1$ subunit was co-expressed with the Ca$_v$ α$_{1B}$ [23]. α$_2$δ up-regulation has been associated with chronic pain and epilepsy, with gabapentin and pregalin binding to α$_2$δ reducing Ca$_v$2.2 trafficking and the symptoms of pain [11]. The α$_2$δ$_{1−3}$, β$_1$, β$_3$ and β$_4$, γ$_1$, γ$_{4−5}$ and γ$_7$ subunits were detected in SH-SY5Y cells

and potentially contribute to the differences in ω-conotoxins potency in whole cell vs. membrane assays.

The γ$_1$ subunit was originally identified in skeletal muscle in complex with Ca$_v$1 channels [52], but effects of this subunit on the ω-conotoxins affinity at Ca$_v$2.2 have not been determined. In contrast, co-expression of the γ$_7$ subunit almost abolished the functional expression of Ca$_v$2.2 in either *Xenopus oocytes* or COS-7 cells [53,54]. The neuronal γ$_2$ is associated with epileptic and ataxic phenotypes of stargazer mouse [55], but was not detected in SH-SY5Y cells. The γ$_5$ and γ$_7$ subunits represent a distinct subdivision of the γ subunit family of proteins identified by structural and sequence homology to stargazing. The γ$_4$ subunit affected only the Ca$_v$2.1 channel [55,56]. The γ$_5$ subunit may be a regulatory subunit of Ca$_v$3.1 channels (for review see: [57]). These subunits may also potentially contribute to differences in ω-conotoxins binding affinities observed in whole cell vs. membrane assays.

While auxiliary subunits affect ω-conotoxin affinity in functional studies, this quaternary complex is likely to be disrupted upon preparation of homogenized membranes for the binding assays [58]. To examine this possibility, we studied the ability of GVIA to displace ^{125}I-GVIA from whole SH-SY5Y cells compared to homogenized membranes. Interestingly, ω-conotoxins CVID, MVIIA and GVIA had higher affinity to displace ^{125}I-GVIA from the homogenized membranes compared to the whole cells,

an effect that was most pronounced for CVID and MVIIA (~100-fold) compared to GVIA (~10-fold). We have previously reported a similar trend for both CVID and MVIIA in heterologous expression system with and without the $\alpha_2\delta$ subunit [22]. Potency estimates obtained with the functional assays were significantly lower than estimates obtained in whole cell radioligand binding assays. The relatively high level of Ca^{2+} in the physiological saline used traditionally for functional assays compared to binding assays could contribute to these differences, since Ca^{2+} non-competitively inhibits ω-conotoxin binding [21]. However, our whole cell data was also obtained by incubating ω-conotoxins in a Ca^{2+}-free physiological saline solution and the origin of these differences is unclear. Interestingly, this effect was most marked for GVIA, intermediate for CVID and insignificant for MVIIA.

In summary, we have characterized functional Ca$_v$ channels expressed in SH-SY5Y human neuroblastoma cell line. Our studies have shown expression of different Ca$_v\alpha$ splice variants, in conjunction with auxiliary subunits in a native context, can modulate the pharmacology of Ca$_v$2.2 channel inhibitors. SH-SY5Y cell line provides a useful model for the investigation of novel human Ca$_v$2.2 inhibitors and is amenable to the establishment of high-throughput assays [59], which can be adapted to detect endogenously expressed human Ca$_v$1.3, Ca$_v$2.2 and possibly Ca$_v$3.1, in the presence of appropriate inhibitors. These assays are expected to prove useful for the discovery and pharmacological characterization of novel Ca$_v$ channel modulators targeting human Ca$_v$ related diseases.

Materials and Methods

Reverse Transcriptase Polymerase Chain Reaction (RT-PCR)

Ca$_v$ channel subtype and auxiliary subunits mRNA expression profiles were investigated in SH-SY5Y cells using standard RT-PCR and specific primers. The primers were designed using The Basic Local Alignment Search Tool (BLAST) [60,61], or otherwise specified as, previously described in the literature. Primer sequences, Gene Bank reference numbers, predicted PCR product sizes, and optimum annealing temperatures are shown in **Table 1**. The primers used to identify Ca$_v$ subtypes and auxiliary subunits were designed so that all splice variants of specific isoforms would be amplified. On the other hand, primers to amplify Ca$_v$2.2 splice variants isoform were designed to be specific to each isoform. PCR conditions to detect splice variants were set as previously described [16,17], with gradient PCR performed for all sets of primers, allowing the identification of optimal annealing temperatures. Different sets of primers were used to identify the full length and isoforms Δ_1 and Δ_2 (see table 1) [16]. These primers were designed based on the region of the domain II-III linker of Ca$_v$2.2 channels, as previously described [16]. Primers used to identify the full length α_{1B1} and short α_{1B2} isoforms were designed based on the C-terminus region [17]. Data is representative of at least three independent experiments.

SH-SY5Y cells (1×10^6) were harvested and total RNA isolated using Trizol® Reagent (Invitrogen, Carlsbad, CA). The isolated RNA was subsequently treated with RNase-free DNase to remove any genomic DNA contamination. RNA concentration was determined by absorbance measurements at 260 nm and its purity/integrity was accessed by analyzing the ratio 260/280 nm with a Nanodrop® (Thermo Scientific). Synthesis of first strand cDNA was performed using 1 μg of the extracted RNA and the Omniscript Reverse Transcription Kit (Qiagen), according to the manufacturer's instructions. cDNA amplifications were performed using Taq Polymerase (New England Biolabs, US). The reaction

mix (total 25 μL) included (μL): 1 cDNA (100 ng), 0.125 of the enzyme, 0.5 reverse and 0.5 forward primers (10 μM), 0.5 dNTPs (10 mM), 2.5 Thermopol reaction buffer (10×) and nuclease free water. RT-PCR was carried through as an initial denaturation step at 95°C for 3 min followed by 35 cycles of the steps: 95°C for 30 s, optimal annealing temperature as previously determined (**Table 1**) for 60 s, 68°C extension for 60 s, plus an extra 5 min elongation step at 68°C. PCR products were analyzed by 1% agarose gel and predicted sizes estimated by comparison with DNA molecular weight makers (50 and 100 bp ladder, New England Biolabs). Target-specific primers for the housekeeping gene GAPDH were designed as previously described [19]. PCR master mix using random primers without cDNA was used as negative gDNA control in all PCRs. Specificity of primers was demonstrated in a range of control experiments (data not shown), including detection of Ca$_v$2.2 plasmid but no other Ca$_v$ subtypes by Ca$_v$2.2 primers; and absence of detectable levels of Ca$_v$2.2 in HEK cells. β_1 and $\alpha_2\delta_1$ primers were positive for β_1 and $\alpha_2\delta_1$ plasmids, while the same primers were negative for β_{2-4} and $\alpha_2\delta_{2-3}$ (data not shown), indicating primers were selective for β_1 and $\alpha_2\delta_1$ auxiliary subunits. In addition, identity of PCR products was further confirmed by sequencing analysis (data not shown). Figures 1A–D is representative of the average of 3–10 individual experiments.

Sequencing

PCR amplicons were first separated on agarose gels and bands of expected sizes identified. PCR products were purified using the Wizard SV Gel and PCR clean-up system (Promega), and a sample of each purified PCR product was sent for sequencing at the Australian Genome Research Facility. cDNA sequences of human Ca$_v$ subtypes and auxiliary subunits were retrieved from GenBank (http://www.ncbi.nlm.nih.gov/Entrez/) and BLASTn [62] was used for confirmation of the identity of human Ca$_v$ subtypes and auxiliary subunits.

Cell Culture

The human neuroblastoma SH-SY5Y cells (Victor Diaz, Goettingen, Germany) were cultured and routinely maintained at 37°C and 5% CO$_2$ in RPMI 1640 antibiotic-free medium (Invitrogen) supplemented with 10% heat-inactivated FBS and 2 mM GlutaMAX^{TM} (Invitrogen). Trypsin/EDTA was used to detach the cells from the T-75 or T175 flasks and cells were split in a ratio of 1:5–1:10 every 3–4 days or when ~80% confluent.

Membrane Preparation for the Radioligand Binding Assay

Radioligand binding assays were performed using rat brain or SH-SY5Y cell membranes prepared as described by Wagner, et al., 1988 [63] with slight modification. For rat brain membranes, male Wistar rats weighing 175–250 g were sacrificed by cervical dislocation and the whole brain was rapidly removed and dissected on ice. At 4°C, tissue was re-suspended in 50 mM HEPES, pH 7.4 (50 mg wet weight tissue/ml buffer), homogenized using a Brinkmann Polytron homogenizer and centrifuged for 15 min at 40,000×g. The pellet was re-suspended in 50 mM HEPES and 10 mM EDTA at pH 7.4, incubated on ice for 30 min and centrifuged at 40,000×g for 10 min. The pellet was then re-suspended in 50 mM HEPES pH 7.4 containing 10% glycerol, aliquots were made and kept at –80°C prior to use. Bicinchoninic acid (BCA) assay reagent (Pierce Rockford, IL) was used for protein quantification.

SH-SY5Y cell membranes were harvested using trypsin/EDTA, washed once with DPBS, and centrifuged for 4 min at 500×g. After centrifugation, the supernatant was discarded and the pellet

re-suspended in 10 ml binding assay buffer at pH 7.2 containing (mM): 20 HEPES, 75 NaCl, 0.2 EDTA, 0.2 EGTA and complete protease inhibitor (Roche Diagnostics, AU) and sonicated. The homogenates were then centrifuged for 30 min at 40,000×g and 4°C. The supernatant was discarded and the pellet dissolved in aliquots of binding assay buffer containing 10% glycerol stored at –80°C prior to use. BCA was used for protein quantification.

Whole Cell Preparation for the Radioligand Binding Assay

Whole cells were prepared as described for SH-SY5Y cell membranes with the following modifications: after cells were harvested and centrifuged, the supernatant was discarded and the pellet re-suspended in sufficient volume of binding buffer to plate 50 µL/well in triplicates in 96 well plates. Specific ω-conotoxins binding was determined using the same concentration of protein as used for SH-SY5Y cell membranes (20 µg/50 µL), corresponds to 600.000 cells per well.

Radioligand Binding Assay

Tyr22-[^{125}I]-GVIA, was prepared using IODOGEN, as previously described by Ahmad [64], purified using reverse phase HPLC and stored at 4°C for use within 3 weeks. On the day of the assay, membranes were thawed on ice and reconstituted to 10 µg/50 µL (rat) or 10–20 µg/50 µL (SH-SY5Y) in binding assay buffer containing 2% complete protease inhibitor and 0.1% bovine serum albumin. Stock [^{125}I]-GVIA was diluted to 20000 cpm/50 µL or 30 pM. For displacement studies, [^{125}I]-GVIA was incubated with rat brain or SH-SY5Y membranes or whole cells and varying concentrations of the competing ligand in triplicates in 96 well plate formats. The plates were incubated with shaking for 1 h at room temperature and vacuum filtered through a glass fiber filter pre-soaked in 0.6% polyethyleneimine (PEI), to reduce non-specific binding and washed with buffer containing (mM) 20 HEPES and 125 NaCl at pH 7.2 using a vacuum system (Tomtec harvester). The filters were then dried at 37°C before being placed in sample bags and soaked in liquid scintillant. Radioactivity was counted using a Microbeta Jet (Wallac, Finland). The non-specific binding was determined in the presence of 50 µL of unlabeled peptides.

Intracellular Ca^{2+} Response Measurement Using the FLIPR

SH-SY5Y cells were seeded onto 96-well or 384-well flat, clear bottom, black-walled imaging plates (Corning, Lowell, MA, US) at a density of 160,000 or 40,000 cells/well, respectively, resulting in 90–95% confluent monolayer after 48 h. On the day of the Ca^{2+} imaging assays, cells were loaded for 30 min in the dark at 37°C with 5 µM Fluo-4 acetomethoxyester (Fluo-4-AM), in physiological salt solution (PSS composition: NaCl 140 mM, glucose 11.5 mM, KCl 5.9 mM, MgCl$_2$ 1.4 mM, NaH$_2$PO$_4$ 1.2 mM, NaHCO$_3$ 5 mM, CaCl$_2$ 1.8 mM, HEPES 10 mM, pH 7.4) containing in addition 0.3% BSA and 10 µM nifedipine. After the incubation period, the cells were washed once with 100 µL assay buffer (no Fluo-4-AM or BSA), and replaced with 100 µL of the same buffer. Plates were then transferred to the FLIPR^{TETRA} (Molecular Devices, Sunnyvale, CA) fluorescent plate image reader, camera gain and intensity were adjusted for each plate to yield between 800–1000 arbitrary fluorescence units (AFU) baseline fluorescence, and Ca^{2+} responses measured using a cooled CCD camera with excitation at 470–495 nM, and emission at 515–575 nM. Ten baseline fluorescence readings were taken prior to the addition of antagonists, and then fluorescent readings every 2 s for 300 s before 90 mM KCl/5 mM CaCl$_2$ buffer was added and fluorescence readings again recorded each second for further 300 s. To ensure full inhibition of Ca$_v$1 responses, the cells were pre-incubated for 40 min with 10 µM nifedipine. To ensure full inhibition of Ca$_v$2.2 responses, the cells were pre-incubated for 10 min with 1–3 µM CVID.

Statistical Analysis

Concentration-response curves were determined following nonlinear regression analysis using a 4-parameter Hill equation, with variable Hill slope fit to the functional assays data and one site fit to the radioligand binding assays; and normalized using GraphPad Prism (Version 5.00, San Diego, California). Negative and positive controls (PSS buffer and KCl 90 mM +5 mM CaCl$_2$, respectively) were used to normalize functional data. All data is presented as mean ± SEM of 6–10 independent experiments performed in triplicate, unless otherwise stated. Statistical significance was determined using analysis of variance (ANOVA) or student's t-test, with statistical significance defined as $p < 0.05$, unless otherwise stated.

Author Contributions

Conceived and designed the experiments: IV RJL. Performed the experiments: SRS IV LR. Analyzed the data: SRS IV LR RJL. Contributed reagents/materials/analysis tools: RJL. Wrote the paper: SRS IV LR RJL.

References

1. Hynd MR, Scott HL, Dodd PR (2004) Glutamate-mediated excitotoxicity and neurodegeneration in Alzheimer's disease. Neurochemistry International 45: 583–595.
2. Alicino I, Giglio M, Manca F, Bruno F, Puntillo F (2012) Intrathecal combination of ziconotide and morphine for refractory cancer pain: A rapidly acting and effective choice. Pain 153: 245–249.
3. Catterall WA (2000) Structure and regulation of voltage-gated Ca^{2+} channels. Annual review of cell and developmental biology 16: 521–555.
4. Feng ZP, Hamid J, Doering C, Bosey GM, Snutch TP, et al. (2001) Residue Gly1326 of the N-type calcium channel alpha 1B subunit controls reversibility of omega-conotoxin GVIA and MVIIA block. J Biol Chem 276: 15728–15735.
5. Catterall WA, Cestele S, Yarov-Yarovoy V, Yu FH, Konoki K, et al. (2007) Voltage-gated ion channels and gating modifier toxins. Toxicon 49: 124–141.
6. Yu FH, Catterall WA (2004) The VGL-chanome: a protein superfamily specialized for electrical signaling and ionic homeostasis. Sci STKE 2004: re15.
7. Lewis RJ, Dutertre S, Vetter I, Christie MJ (2012) Conus venom peptide pharmacology. Pharmacol Rev 64: 259–298.
8. Catterall WA, Goldin AL, Waxman SG (2003) International Union of Pharmacology. XXXIX. Compendium of voltage-gated ion channels: sodium channels. Pharmacological reviews 55: 575–578.
9. Catterall WA (2011) Voltage-gated calcium channels. Cold Spring Harbor Perspectives in Biology 3.
10. Olivera BM, Miljanich GP, Ramachandran J, Adams ME (1994) Calcium channel diversity and neurotransmitter release: the omega-conotoxins and omega-agatoxins. Annu Rev Biochem 63: 823–867.
11. Dolphin AC (2009) Calcium channel diversity: multiple roles of calcium channel subunits. Curr Opin Neurobiol 19: 237–244.
12. Arikkath J, Campbell KP (2003) Auxiliary subunits: essential components of the voltage-gated calcium channel complex. Curr Opin Neurobiol 13: 298–307.
13. Reeve HL, Vaughan PFT, Peers C (1994) Calcium Channel Currents in Undifferentiated Human Neuroblastoma (SH-SY5Y) Cells: Actions and Possible Interactions of Dihydropyridines and ω-Conotoxin. European Journal of Neuroscience 6: 943–952.
14. Reuveny E, Narahashi T (1993) Two types of high voltage-activated calcium channels in SH-SY5Y human neuroblastoma cells. Brain Res 603: 64–73.
15. Vaughan PFT, Peers C, Walker JH (1995) The use of the human neuroblastoma SH-SY5Y to study the effect of second messengers on noradrenaline release. General Pharmacology: The Vascular System 26: 1191–1201.
16. Kaneko S, Cooper CB, Nishioka N, Yamasaki H, Suzuki A, et al. (2002) Identification and characterization of novel human Ca$_v$2.2 (alpha 1B) calcium channel variants lacking the synaptic protein interaction site. J Neurosci 22: 82–92.

17. Williams ME, Brust PF, Feldman DH, Patthi S, Simerson S, et al. (1992) Structure and functional expression of an omega-conotoxin-sensitive human N-type calcium channel. Science 257: 389–395.

18. Szabo Z, Obermair GJ, Cooper CB, Zamponi GW, Flucher BE (2006) Role of the synprint site in presynaptic targeting of the calcium channel Ca$_v$2.2 in hippocampal neurons. European Journal of Neuroscience 24: 709–718.

19. Chiou W-F (2006) Effect of Aβ exposure on the mRNA expression patterns of voltage-sensitive calcium channel α1 subunits (α1A–α1D) in human SK-N-SH neuroblastoma. Neurochem Int 49: 256–261.

20. Schroeder CI, Lewis RJ (2006) ω-conotoxins GVIA, MVIIA and CVID: SAR and clinical potential. Marine Drugs 4: 193–214.

21. Lewis RJ, Nielsen KJ, Craik DJ, Loughnan ML, Adams DA, et al. (2000) Novel ω-conotoxins from Conus catus discriminate among neuronal calcium channel subtypes. Journal of Biological Chemistry 275: 35335–35344.

22. Mould J, Yasuda T, Schroeder CI, Beedle AM, Doering CJ, et al. (2004) The alpha2delta auxiliary subunit reduces affinity of omega-conotoxins for recombinant N-type (Ca$_v$2.2) calcium channels. J Biol Chem 279: 34705–34714.

23. Berecki G, Motin L, Haythornthwaite A, Vink S, Bansal P, et al. (2010) Analgesic (omega)-conotoxins CVIE and CVIF selectively and voltage-dependently block recombinant and native N-type calcium channels. Mol Pharmacol 77: 139–148.

24. Benjamin ER, Pruthi F, Olanrewaju S, Shan S, Hanway D, et al. (2006) Pharmacological characterization of recombinant N-type calcium channel (Ca$_v$2.2) mediated calcium mobilization using FLIPR. Biochem Pharmacol 72: 770–782.

25. Dai G, Haedo RJ, Warren VA, Ratliff KS, Bugianesi RM, et al. (2008) A high-throughput assay for evaluating state dependence and subtype selectivity of Ca$_v$2 calcium channel inhibitors. Assay Drug Dev Technol 6: 195–212.

26. Finley MF, Lubin ML, Neeper MP, Beck E, Liu Y, et al. (2010) An integrated multiassay approach to the discovery of small-molecule N-type voltage-gated calcium channel antagonists. Assay Drug Dev Technol 8: 685–694.

27. Furukawa T, Yamakawa T, Midera T, Sagawa T, Mori Y, et al. (1999) Selectivities of dihydropyridine derivatives in blocking Ca^{2+} channel subtypes expressed in Xenopus oocytes. J Pharmacol Exp Ther 291: 464–473.

28. Nowycky MC, Fox AP, Tsien RW (1985) Three types of neuronal calcium channel with different calcium agonist sensitivity. Nature 316: 440–443.

29. Trombley P, Westbrook G (1991) Voltage-gated currents in identified rat olfactory receptor neurons. The Journal of Neuroscience 11: 435–444.

30. Motin L, Yasuda T, Schroeder CI, Lewis RJ, Adams DJ (2007) w-Conotoxin inhibition of excitatory synaptic transmission evoked by dorsal root stimulation in rat superficial dorsal horn-conotoxin CVIB differentially inhibits native and recombinant N- and P/Q-type calcium channels. Eur J Neurosci 25: 435–444.

31. Alvarez Maubecin V, Sanchez VN, Rosato Siri MD, Cherksey BD, Sugimori M, et al. (1995) Pharmacological characterization of the voltage-dependent Ca^{2+} channels present in synaptosomes from rat and chicken central nervous system. J Neurochem 64: 2544–2551.

32. Martin RL, Lee JH, Cribbs LL, Perez-Reyes E, Hanck DA (2000) Mibefradil block of cloned T-type calcium channels. J Pharmacol Exp Ther 295: 302–308.

33. Viana F, Van Den Bosch L, Missiaen L, Vandenberghe W, Droogmans G, et al. (1997) Mibefradil (Ro 40m5967) blocks multiple types of voltage-gated calcium channels in cultured rat spinal motoneurones. Cell Calcium 22: 299–311.

34. Arnoult C, Villaz M, Florman HM (1998) Pharmacological properties of the T-type Ca^{2+} current of mouse spermatogenic cells. Mol Pharmacol 53: 1104–1111.

35. Todorovic SM, Lingle CJ (1998) Pharmacological properties of T-type Ca^{2+} current in adult rat sensory neurons: effects of anticonvulsant and anesthetic agents. J Neurophysiol 79: 240–252.

36. Cizkova D, Marsala J, Lukacova N, Marsala M, Jergova S, et al. (2002) Localization of N-type Ca^{2+} channels in the rat spinal cord following chronic constrictive nerve injury. Exp Brain Res 147: 456–463.

37. Wallace MS, Rauck RL, Deer T (2010) Ziconotide combination intrathecal therapy: rationale and evidence. Clin J Pain 26: 635–644.

38. Lambert DG, Whitham EM, Baird JG, Nahorski SR (1990) Different mechanisms of Ca^{2+} entry induced by depolarization and muscarinic receptor stimulation in SH-SY5Y human neuroblastoma cells. Molecular Brain Research 8: 263–266.

39. Williams ME, Feldman DH, McCue AF, Brenner R (1992) Structure and functional expression of alpha 1, alpha 2, and beta subunits of a novel human neuronal calcium channel subtype. Neuron (Cambridge, Mass) 8: 71–84.

40. Xie X, Van Deusen AL, Vitko I, Babu DA, Davies LA, et al. (2007) Validation of high throughput screening assays against three subtypes of Ca(v)3 T-type channels using molecular and pharmacologic approaches. Assay Drug Dev Technol 5: 191–203.

41. Bezprozvanny I, Tsien RW (1995) Voltage-dependent blockade of diverse types of voltage-gated Ca^{2+} channels expressed in Xenopus oocytes by the Ca^{2+} channel antagonist mibefradil (Ro 40–5967). Mol Pharmacol 48: 540–549.

42. Bell TJ, Thaler C, Castiglioni AJ, Helton TD, Lipscombe D (2004) Cell-Specific Alternative Splicing Increases Calcium Channel Current Density in the Pain Pathway. Neuron 41: 127–138.

43. Sonnier H, Kolomytkin OV, Marino AA (2000) Resting potential of excitable neuroblastoma cells in weak magnetic fields. Cell Mol Life Sci 57: 514–520.

44. Nielsen KJ, Schroeder T, Lewis R (2000) Structure-activity relationships of omega-conotoxins at N-type voltage-sensitive calcium channels. J Mol Recognit 13: 55–70.

45. Lipscombe D, Pan JQ, Gray AC (2002) Functional diversity in neuronal voltage-gated calcium channels by alternative splicing of Ca(v)alpha1. Mol Neurobiol 26: 21–44.

46. Lipscombe D, Raingo J (2007) Alternative splicing matters: N-type calcium channels in nociceptors. Channels (Austin) 1: 225–227.

47. Lin Z, Haus S, Edgerton J, Lipscombe D (1997) Identification of functionally distinct isoforms of the N-type Ca^{2+} channel in rat sympathetic ganglia and brain. Neuron 18: 153–166.

48. Brust PF, Simerson S, McCue AF, Deal CR, Schoonmaker S, et al. (1993) Human neuronal voltage-dependent calcium channels: studies on subunit structure and role in channel assembly. Neuropharmacology 32: 1089–1102.

49. Zamponi GW, McCleskey EW (2004) Splicing it up: a variant of the N-type calcium channel specific for pain. Neuron 41: 3–4.

50. Maximov A, Bezprozvanny I (2002) Synaptic targeting of N-type calcium channels in hippocampal neurons. J Neurosci 22: 6939–6952.

51. Jimenez C, Bourinet E, Leuranguer V, Richard S, Snutch TP, et al. (2000) Determinants of voltage-dependent inactivation affect Mibefradil block of calcium channels. Neuropharmacology 39: 1–10.

52. Sandoval A, Arikkath J, Monjaraz E, Campbell KP, Felix R (2007) Gamma1-dependent down-regulation of recombinant voltage-gated Ca^{2+} channels. Cellular and molecular neurobiology 27: 901–908.

53. Moss FJ, Viard P, Davies A, Bertaso F, Page KM, et al. (2002) The novel product of a five-exon stargazin-related gene abolishes Ca$_v$2.2 calcium channel expression. EMBO J 21: 1514–1523.

54. Ferron L, Davies A, Page KM, Cox DJ, Leroy J, et al. (2008) The stargazin-related protein gamma 7 interacts with the mRNA-binding protein heterogeneous nuclear ribonucleoprotein A2 and regulates the stability of specific mRNAs, including Ca$_v$2.2. J Neurosci 28: 10604–10617.

55. Kang MG, Chen CC, Felix R, Letts VA, Frankel WN, et al. (2001) Biochemical and biophysical evidence for gamma 2 subunit association with neuronal voltage-activated Ca^{2+} channels. J Biol Chem 276: 32917–32924.

56. Sharp AH, Black JL, 3rd, Dubel SJ, Sundarraj S, Shen JP, et al. (2001) Biochemical and anatomical evidence for specialized voltage-dependent calcium channel gamma isoform expression in the epileptic and ataxic mouse, stargazer. Neuroscience 105: 599–617.

57. Lacinova L (2005) Voltage-dependent calcium channels. Gen Physiol Biophys 24 Suppl 1: 1–78.

58. Dold KM, Greenlee WF (1990) Filtration assay for quantitation of 2,3,7,8-tetrachlorodibenzo-p-dioxin (TCDD) specific binding to whole cells in culture. Anal Biochem 184: 67–73.

59. Vetter I, Mozar CA, Durek T, Wingerd JS, Alewood PF, et al. (2012) Characterisation of Nav types endogenously expressed in human SH-SY5Y neuroblastoma cells. Biochemical Pharmacology 83: 1562–1571.

60. Maximov A, Bezprozvanny I (2002) Synaptic Targeting of N-Type Calcium Channels in Hippocampal Neurons. The Journal of Neuroscience 22: 6939–6952.

61. Altschul SF, Gish W, Miller W, Myers EW, Lipman DJ (1990) "Basic local alignment search tool" J. Mol. Biol. 403–410.

62. Ye J, Coulouris G, Zaretskaya I, Cutcutache I, Rozen S, et al. (2012) Primer-BLAST: A tool to design target-specific primers for polymerase chain reaction. BMC Bioinformatics 13: 134.

63. Wagner J, Snowman A, Biswas A, Olivera B, Snyder S (1988) ω- conotoxin GVIA binding to a high affinity receptor in brain: Characterization, calcium sensitivity and Solubilization. The Journal of Neuroscience 9: 3354–3359.

64. Ahmad S, Miljanich G (1988) The calcium channel antagonist, omega-conotoxin, and electric organ nerve terminals: binding and inhibition of transmitter release and calcium influx. 453: 247–256.